

Anatomy of endemic amphipods (Crustacea: Amphipoda) from Lake Baikal in light of implanting optical sensors

Ekaterina P. Shchapova^{1,2}, Yaroslav A. Rzhechitskiy¹,
Olga V. Kaluzhnaya¹, Evgeniy A. Titov³, Igor V. Khanaev⁴,
Kseniya P. Vereshchagina¹, Maxim A. Timofeyev¹,
Anton N. Gurkov^{1,2*}

¹ Institute of Lake Baikal Biology, Irkutsk State University, Lenin st. 3, Irkutsk 664025 Russia.

² Baikal Research Centre, Rabochaya st. 5v, Irkutsk 664003 Russia.

³ East-Siberian Institute of Medical and Ecological Research, Mikrorayon 12a 3, Angarsk 665827 Russia.

⁴ Limnological Institute of the Siberian Branch of the Russian Academy of Sciences, Ulan-Batorskaya st. 3, Irkutsk 664033 Russia.

* Corresponding author

Ekaterina Shchapova: shchapova.katerina@gmail.com <https://orcid.org/0000-0001-9084-7675>

Yaroslav Rzhechitskiy: rzhechitskiy.yar@gmail.com <https://orcid.org/0000-0001-8603-572X>

Olga Kaluzhnaya: olgavk101010@gmail.com <https://orcid.org/0000-0002-3845-6375>

Evgeniy Titov: evgtitov83@gmail.com <https://orcid.org/0000-0002-0665-8060>

Igor Khanaev: igkhan@lin.irk.ru <https://orcid.org/0000-0001-6431-2765>

Kseniya Vereshchagina: k.p.vereshagina@gmail.com <https://orcid.org/0000-0002-4843-5287>

Maxim Timofeyev: m.a.timofeyev@gmail.com <https://orcid.org/0000-0002-5250-6818>

Anton Gurkov: a.n.gurkov@gmail.com <https://orcid.org/0000-0002-8390-1570>

ABSTRACT: Implantable devices for continuous release or sensing of specific substances inside animal tissues have the potential to facilitate automatization of research on a multitude of species. However, injection of implants requires understanding of the species anatomies in order to ensure a proper contact with the chosen tissues and prevent damage of internal organs. Here, we dive into the unclear aspects of the anatomy of amphipods (Crustacea: Amphipoda), one of the most important groups of crustaceans, on the example of morphologically diverse endemic amphipods from Lake Baikal. In particular, we searched for large lacunae in frozen sections of a relatively small shallow-water amphipod (~3 cm long) and tested the applicability of optical sensors close to the body surface of larger deeper-dwelling species (over 6 cm long) with outgrowths of exoskeleton. Apical muscles were found to be the most universal site for application of implantable optical sensors not only in smaller species but also in larger amphipods. For the cases when the implants should have direct contact with animal hemolymph, we identified a suitable large lacuna in the segments 9-10 on the example of a shallow-water *Eulimnogammarus verrucosus*. As a by-product, we found dorsal carinae of the largest Baikal amphipods of the genus *Acanthogammarus* to contain a significant amount of adipose-like tissue.

How to cite this article: Shchapova E.P., Rzhechitskiy Y.A., Kaluzhnaya O.V., Titov E.A., Khanaev I.V., Vereshchagina K.P., Timofeyev M.A., Gurkov A.N. 2026. Anatomy of endemic amphipods (Crustacea: Amphipoda) from Lake Baikal in light of implanting optical sensors // Invert. Zool. Vol.23. No.1. P.100–113. doi: 10.15298/invertzool.23.1.06

KEY WORDS: autofluorescence; Baikal; crustaceans; cryotomy; deep-water; implantable sensors.

Анатомия эндемичных байкальских амфипод (Crustacea: Amphipoda) в свете имплантации оптических сенсоров

Е.П. Щапова^{1,2}, Я.А. Ржечицкий¹, О.В. Калюжная¹, Е.А. Титов³,
И.В. Ханаев⁴, К.П. Верещагина¹, М.А. Тимофеев¹, А.Н. Гурков^{1,2*}

¹ НИИ биологии Байкала, Иркутский государственный университет, ул. Ленина 3, Иркутск 664025 Россия.

² Байкальский исследовательский центр, ул. Рабочая 5в, Иркутск 664003 Россия.

³ ФГБНУ Восточно-Сибирский институт медико-экологических исследований, микрорайон 12а 3, Ангарск 665827 Россия.

⁴ Лимнологический институт СО РАН, ул. Улан-Баторская 3, Иркутск 664033 Россия.

* Ответственный за переписку: a.n.gurkov@gmail.com

РЕЗЮМЕ: В настоящее время ведётся разработка широкого ряда имплантируемых устройств для целевой доставки или непрерывного мониторинга содержания разнообразных веществ в тканях животных, что может способствовать повышению автоматизации исследований в области физиологии животных. Однако введение имплантов требует понимания анатомии объектов исследования для обеспечения его контакта только с выбранной тканью и минимизации вероятности повреждения внутренних органов. В контексте введения оптических сенсоров в данной работе проведена оценка анатомии амфипод (Crustacea: Amphipoda), одной из наиболее значимых групп ракообразных, на примере морфологически разнообразных эндемичных амфипод озера Байкал. Для этого проведён поиск крупных лакун на криотомных срезах тела относительно небольших прибрежных амфипод (длина тела ~3 см). Кроме того, проверена применимость оптических сенсоров вблизи поверхности тела более крупных видов (длиной более 6 см) с выростами экзоскелета, населяющих большие глубины. Установлено, что спинные мышцы являются наиболее универсальной точкой введения имплантируемых оптических сенсоров как для небольших видов, так и для крупных амфипод. Для случаев, когда имплант должен иметь прямой контакт с гемолимфой, подходящей точкой введения оказалась крупная лакуна в сегментах 9–10, обнаруженная на примере литорального вида *Eulimnogammarus verrucosus*. Дополнительно, в спинном киле двух видов байкальских амфипод рода *Acanthogammarus* было обнаружено значительное количество жироподобной ткани.

Как цитировать эту статью: Shchapova E.P., Rzhechitskiy Y.A., Kaluzhnaya O.V., Titov E.A., Khanaev I.V., Vereshchagina K.P., Timofeyev M.A., Gurkov A.N. 2026. Anatomy of endemic amphipods (Crustacea: Amphipoda) from Lake Baikal in light of implanting optical sensors // *Invert. Zool.* Vol.23. No.1. P.100–113. doi: 10.15298/invertzool.23.1.06

КЛЮЧЕВЫЕ СЛОВА: автофлуоресценция, Байкал, глубоководная зона, имплантируемые сенсоры, криотомия, ракообразные.

Introduction

Crustaceans are a significant group of invertebrates widespread in both aquaculture and natural environments (Rabet, 2021). However, comprehensive physiological studies on the multitude of species of economical or environmental importance are laborious and time-consuming, especially on small crustaceans. Currently, various implantable devices are being developed and may soon simplify and automatize physiological research on different objects, including aquatic animals (Li *et al.*, 2021; Rzhechitskiy *et al.*, 2022; Hu *et al.*, 2024; Madhu *et al.*, 2024). Relatively simple implants can already be used for a slow release of loaded compounds into animal tissues (McCallum *et al.*, 2019), which offers simplification of experimental treatments in ecotoxicological research and may be beneficial for continuous drug or hormone release in aquaculture. The implantable microelectronic sensors (Sonmezoglu *et al.*, 2021; Gudlavalleti *et al.*, 2023) may allow long-term dynamic monitoring of critical biochemical parameters without the need in repetitive blood samplings or similar handling procedures. Another popular approach for determination of biochemical parameters in animal blood or interstitial fluid involves implants carrying some sensitive components capable of transducing their signal via light without microelectronic parts (Kanick *et al.*, 2019; Ehrlich *et al.*, 2021; Kaefer *et al.*, 2021; Shchapova *et al.*, 2022; Ivich *et al.*, 2023). The sensitive component can be of various nature from fluorescent dyes detecting specific ions to larger complexes involving, e.g., aptamers selectively binding certain molecules and requires an external device for acquiring and analyzing the signal encoded in the light spectrum or temporal pattern. The advantages of these optical sensors are simple preparation and miniaturization down to microns in size, which is especially important for small animals such as many species of crustaceans.

Introduction and application of the implants inside animal tissues requires good understanding of the body structure and its variation during movements and depending on the such factors as season or sex. This is necessary in order to (i) keep the internal organs undamaged during the injection and (ii) ensure the proper contact with the chosen tissue and preferably only with

this tissue. The tissue of interest is usually blood/hemolymph or muscle, and the safe procedure for implant injection into either depends on the anatomy of the species. Another important factor, particularly in the case of microelectronics-free sensors, is optical properties of different organs since autofluorescence or poor light transmittance can significantly complicate the signal acquisition and analysis in certain body parts.

Amphipods (Crustacea: Amphipoda) are one of the most species-rich orders of crustaceans with approximately 10,000 species described that colonized immense variety of ecological niches with mostly benthic forms, benthopelagic representatives, some pelagic species, animals that flourish in forest litter, and a few species that live as commensals or parasites (Ahyong *et al.*, 2011; Bellan-Santini, 2015; Bhoi *et al.*, 2023). The variability in niches dictates a corresponding variability in body sizes and forms. A substantial part of the possible morphological diversity of amphipods in general is nicely represented in just one waterbody, ancient Lake Baikal, with its over 350 species and subspecies of endemic amphipods (Takhteev, 2000; Takhteev *et al.*, 2015; Drozdova *et al.*, 2020). Most littoral species in Baikal are typical benthic forms of variable size up to 4 cm long with smooth, protrusion-free bodies. However, the bodies of deeper-dwelling animals may be much larger and distinguished by outgrowths of exoskeleton, such as knolls, ridges, carina, spines, denticles, and so forth, which are sometimes observed on the sides and sometimes on the sagittal dorsal line of all or some of the segments (Kozhov, 1963).

The anatomy of amphipods has been the subject of extensive research for a long time (Schmitz, 1967) with the majority of studies focusing on specific organs or systems, such as the nervous and excretory systems (Wirkner, Richter, 2007; Hyne, 2011; Mekhanikova *et al.*, 2012; Ramm, Scholtz, 2017; Wittfoth *et al.*, 2019). However, most of the studies employed tissue dehydration techniques in analyzing overall body structure, which could substantially reduce the hemolymph-filled spaces between the organs during the sample preparation and result in the organs becoming more closely aligned before sectioning and visualization. This can be critical for planning the injections of implant that should have the direct contact with amphipod hemolymph. Moreover, the

information about internal anatomy of larger amphipod species, especially the ones carrying exoskeleton outgrowths, is almost absent. At the same time, we found littoral *Eulimnogammarus verrucosus* (Gerstfeldt, 1858) and other amphipods from Lake Baikal to be convenient models for developing implantable optical sensors for crustaceans of different sizes (Gurkov *et al.*, 2016, 2018; Nazarova *et al.*, 2023).

In this study we aimed at obtaining more information about anatomy and optical properties of different organs for applying implants in bodies of endemic amphipods from Lake Baikal. In particular, we asked the main questions whether (i) benthic littoral species have significant hemolymph-filled spaces between their organs, (ii) optical sensors can be readily visualized under the thick exoskeleton of larger amphipods and (iii) exoskeleton outgrowths of the larger amphipods contain live tissues. The last question was raised since the outgrowths may be a convenient injection site where the implant can be easily found. The first question was addressed again on the example of *E. verrucosus* as one of the largest littoral species, while the second and the third were applied to deeper-dwelling larger *Acanthogammarus victorii* (Dybowsky, 1874) and *Acanthogammarus (Brachyuropus) grewingkii* (Dybowsky, 1874) with similar morphology.

Material and methods

Animal Sampling and Maintenance

All experimental procedures with amphipods were conducted in accordance with the EU Directive 2010/63/EU for animal experiments and were approved by the Animal Subjects Research Committee of the Institute of Biology at Irkutsk State University (the protocol #10/2022). All studied species are not endangered nor protected. The species were determined according to the keys by (Bazikalova, 1945; Takhteev, 2000).

Precopulas of *E. verrucosus* with animal sizes of approximately 25–35 mm in length were collected using a hand net (kick sampling) in the littoral zone of Lake Baikal in the vicinity of the Listvyanka village at depths of 0.01–1.2 m. The animals were transported to the laboratory and kept in 2.5-L-aquaria with continuous aeration at approximately 6 °C for several days before further procedures. For cryosectioning, males and females were separated and frozen in liquid nitrogen. Individuals of *A. grewingkii* (~60–70 mm long) were obtained by trawling from 300 to 1450 m in the Central and Southern basins of Lake Bai-

kal. The animals were frozen in liquid nitrogen for cryosectioning or fixed for histological analysis (see details below) right after capture. *A. victorii* (~65–70 mm long) was sampled by divers near the Bolshie Koty settlement on the shoreline of Lake Baikal from depths of 8–16 m. The amphipods were kept in the laboratory conditions at 4 °C in a 30-L-aquarium with constant aeration for 52 days before implanting fluorescent sensors or other analyses. The animals were fed every two weeks. Lengths of animals from rostrum to telson were determined by photos using ImageJ v.1.52a (Schneider *et al.*, 2012).

Frozen sectioning and visualization

Five animals of *A. grewingkii*, five individuals of *A. victorii* and 40 animals of *E. verrucosus* have been used to analyze the anatomy of these species. Amphipods were subjected to frozen sectioning following their shock freezing in liquid nitrogen. On the day prior to cryosectioning, the amphipods were transferred from liquid nitrogen to a temperature of –30 °C in order to facilitate the cutting of samples. Before placement in the cryostat, amphipods were fixed in a matrix cryotomy medium Tissue-Tek O.C.T. Compound (Sakura Finetek, USA) on a holder. Longitudinal cryosections (30 µm thickness) of amphipods were obtained with HM525 NX cryostat (Thermo Fisher Scientific, Germany) at –15 °C. A part of the cryosections was stained with hematoxylin and eosin as described below (see the next section). The cryosections were captured by an EOS 1200D camera (Canon, Japan) either alone or in combination with a Z16 APO macroscope (Leica Microsystems, Germany). Transverse cryosections were obtained by cutting the samples with scalpel (without the embedding medium; 1–3 mm thick sections were removed at each step) in the direction from the head to the urosome and were visualized under an SPM0880 zoom stereomicroscope (Altami, Russia); both stages were performed at –5 °C. Image correction and, if necessary, image stitching were conducted using GIMP v.2.10.20 (<https://www.gimp.org>); figures were prepared using Inkscape v.1.0.2 (<https://inkscape.org>). Autofluorescence imaging of internal organs and exoskeleton of *E. verrucosus* was performed on transverse cryosections using a Celena S inverted microscope (Logos Biosystems, the Republic of Korea). The obtained images are available in the open repository: https://figshare.com/projects/Anatomy_of_endemic_amphipods_from_Lake_Baikal/223560.

Paraffin sectioning and visualization

Individuals of *A. grewingkii* ($n = 3$) and *A. victorii* ($n = 4$) were fixed prior to histological analysis by the following steps. Approximately 0.1 mL of Davidson's solution (ethanol, 95%, 1200 ml; formaldehyde, 37%, 800 ml; tap water, 1200 ml; glacial acetic acid, 400 ml) was injected into the central vessel using a medi-

cal syringe with a 16G (0.6 mm) needle. Immediately after the injection, the urosome was excised, and the crustacean was fully immersed in Davidson's solution for further fixation. The samples were stored at 25 °C for a period of between one day and five months.

Fixed amphipods were divided into segments and immersed in Isoprep solution (HP-IS-AL05, BioVitrum, Russia) three times for 15 min, after which they were placed in paraffin (BioVitrum, Russia) three times for 30 minutes at 65 °C. The paraffin molds were sectioned with a thickness of 6 µm using S700 microtome (RWD, China). The sections were deparaffinized after three times in xylene for 5 min, two times in Isoprep solution for 5 min and placing in tap water for 10 min. Finally, the sections were stained with hematoxylin and eosin (H&E) with the following liquids: solution of Mayer's hematoxylin (HK-G0-DD05, BioVitrum, Russia) for 2–3 min, tap water for 5 min, alcohol eosin solution (HK-ES-BL01, BioVitrum, Russia) for 1 min, 96 % ethanol for 5 min, Isoprep two times for 1 min, xylene 5–10 min and VitroGel (12-005/250, Biovitrum, Russia). The stained sections were observed under upright DMLB microscope (Leica Microsystems, Germany) equipped with a 20 megapixel digital color camera (Lacopa, Russia). Image correction was conducted using GIMP v.2.10.20 (<https://www.gimp.org>). Obtained images are available in the open repository: https://figshare.com/projects/Anatomy_of_endemic_amphipods_from_Lake_Baikal/223560.

Preparation and injection of pH sensors

As the model implantable sensor for testing translucency of *A. victorii* exoskeleton, we used hydrogel fibers carrying the dye seminaphtharhodafluor-1 (SNARF-1) changing its fluorescence color in response to shifts in the solution pH. The sensor was prepared by mixing 27.5 µL of 1.2 mg/mL SNARF-1 conjugated with dextran (D-3304, Thermo Fisher Scientific, MA, USA), 10 µL of distilled water, 30 µL of the solution containing 30% acrylamide (A1089, AppliChem, Germany) and 0.8% N,N'-methylenebisacrylamide (A3636, AppliChem, Germany), 0.5 µL N,N,N',N'-tetramethylethylenediamine (Acros-13845, Acros Organics, Belgium), and 1 µL of 10% ammonium persulfate solution. Once the mixture was combined and mixed, it was transferred into glass capillaries with an internal diameter of approximately 0.3 mm for several minutes. Following polymerization, the polyacrylamide gels were manually extracted from the capillaries and incubated in distilled water for two to five hours to remove any unpolymerized components.

The injection of the gels of approximately 1–2 mm in length into amphipod tissues was performed using 16G hypodermic needles (SF Medical Products GmbH, Germany). A piece of thin fishing line was used as the plunger to keep the sensor in tissue after the needle was introduced and removed.

Spectroscopy of amphipods

All analyses described in this section were performed strictly on alive and active individuals to imitate the conditions of laboratory physiological experiments on the study objects. Sensor fluorescence and autofluorescence of *E. verrucosus* ($n = 4$) and *A. victorii* ($n = 3$) were visualized under the Z16 APO microscope (Leica Microsystems, Germany) with a fiber spectrometer QE Pro (OceanOptics, FL, USA; INTSMA-200 optical slit, 350–1100 nm wavelengths range, QP400-2-VIS-NIR optical fiber) attached to the photo port for recording the spectra. The red channel, which has a peak excitation wavelength of 520 nm and a long-pass emission filter transmitting from approximately 590 nm, was employed for fluorescence excitation. The software package Scilab v5.5.2 (<https://www.scilab.org>) was employed for analysis of the acquired spectra. Individuals of *E. verrucosus* were maintained under the microscope using a thermostatic chamber containing circulating Baikal water at the temperature of 5–8 °C as previously described (Gurkov *et al.*, 2018). *A. victorii* was placed under the microscope in a Petri dish containing Baikal water, and the temperature control and water exchange were performed manually.

Results

Structure of pereon and pleon of *Eulimnogammarus verrucosus*

In this study, one of the primary goals was to assess the natural dimensions of the spaces filled with hemolymph between the organs in different areas of the littoral amphipod body in order to identify the optimal size, shape, and possible insertion ways for implants. Specifically for this task we utilized native frozen sections on *E. verrucosus*, which has generally smooth body but also some spines and setae on pleon.

The typical structure of sexually mature adults of *E. verrucosus* is shown in Fig. 1. Depending on its function, the implant should mostly be in contact with muscles or hemolymph, and here we focused the analysis around these two options.

The muscles on the dorsal part of benthic amphipods are typically most convenient for injection and visualization of implants, and longitudinal sections of *E. verrucosus* revealed that the apical muscles are the largest in the segments from the sixth to the tenth (Fig. 1A,C). Moreover, the cross sections (Fig. 1B) suggest the muscles are even more developed slightly to the sides from the sagittal body plane, which

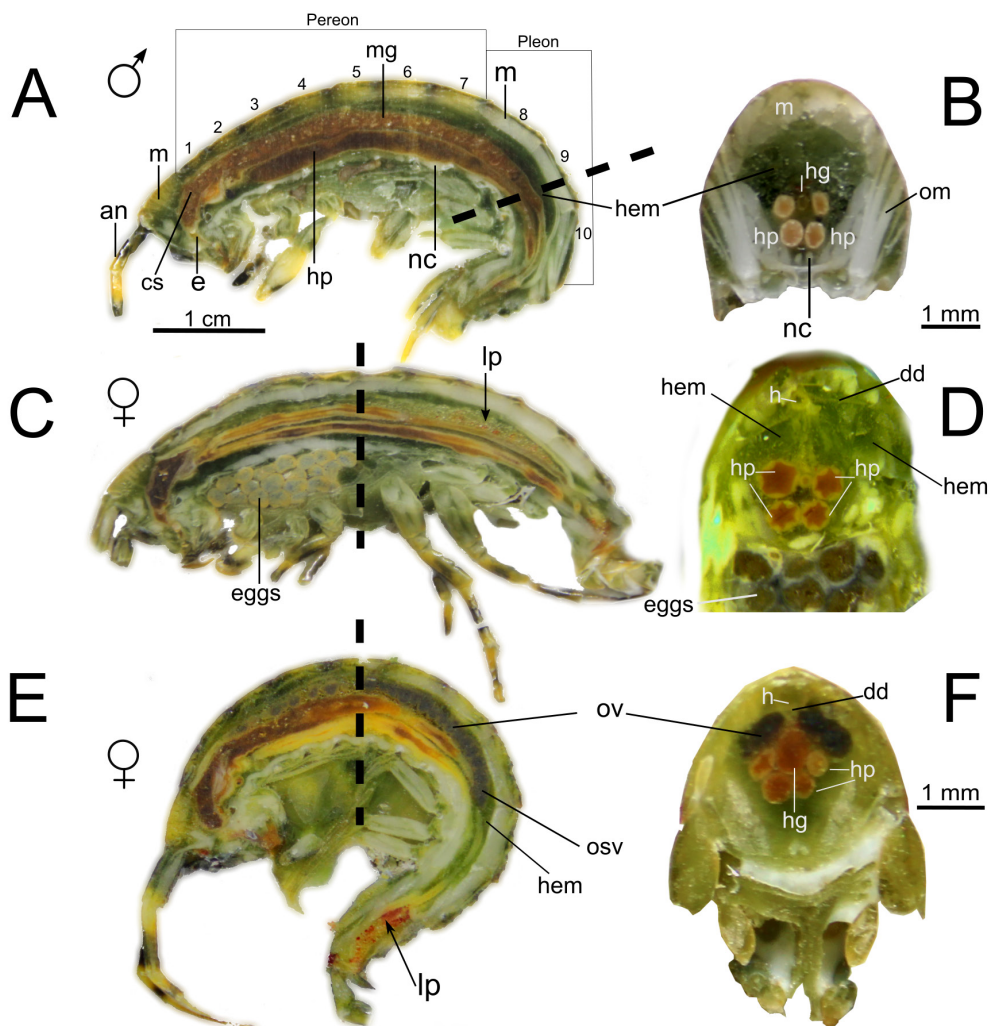


Fig. 1. Cryosections of the littoral amphipod *Eulimnogammarus verrucosus* ($n = 32$). A — lateral view at the anatomical structures of a male; B — transversal section of male pleon at 9th segment; C, E — lateral view at the anatomical structures of females at different stages of reproduction; D, F — transversal sections of female pereon at 5th and 6th segments respectively at different stages of reproduction. The dashed lines on A, C and E show the respective cross sections on B, D and F.

Abbreviations: an — antenna; cs — cardiac stomach; dd — dorsal diaphragm; e — esophagus; h — lumen of the heart; hem — hemolymph; hg — hind-gut; hp — hepatopancreas; lp — lipid droplets; mg — mid-gut; nc — nerve cord; m — muscle; osv — oocyte in secondary vitellogenesis; ov — ovary.

is supported by H&E staining of the respective longitudinal section of *E. verrucosus* (Fig. 2).

We found a number of significant hemolymph-filled spaces on cryosections of *E. verrucosus*. Amphipods have a dorsal pulsatile heart that is connected to the anterior and posterior aortae in the body axis to form the hemolymph

vascular system. The posterior aorta is connected to the dorsal diaphragm and descends into the pereon, or abdomen, as a straight tube (Fig. 1D). Together with the diaphragm the apical muscles form a lacuna due to their association with exoskeleton (Fig. 1D). The hepatopancreas ducts are situated in close proximity to the

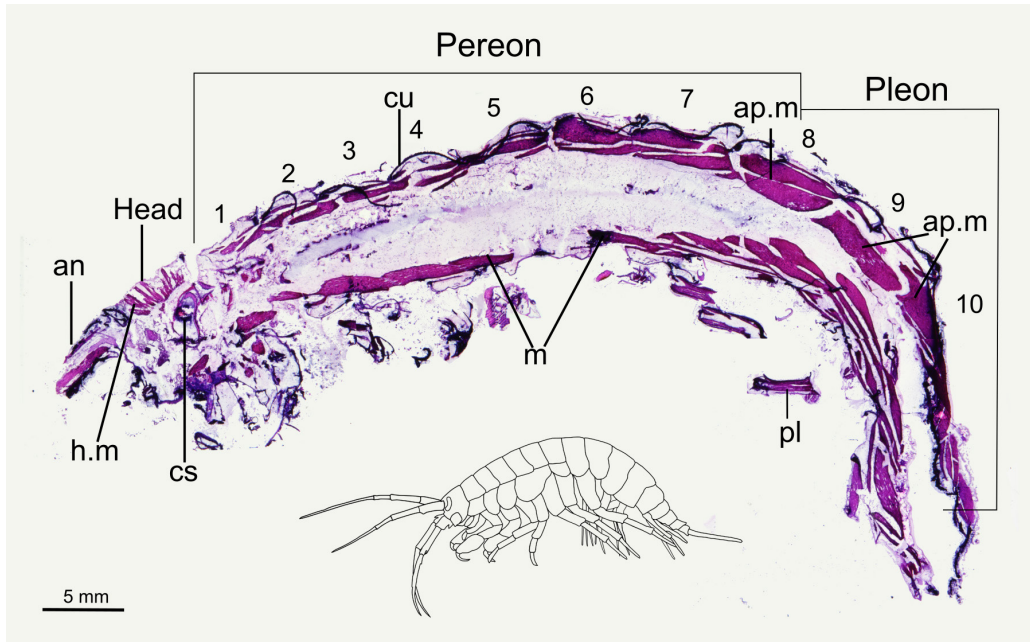


Fig. 2. H&E stained longitudinal cryosection showing anatomical structures to the side from the sagittal body plane of *Eulimnogammarus verrucosus*.

Abbreviations: an — antenna; ap.m — apical muscles; cs — cardiac stomach; cu — cuticle; h.m — head muscles; m — muscles; pl — pleopod.

intestine, which is located medially, while the basal muscles, similarly to the apical ones, are also attached to cuticle. From the second to the seventh segment, a hemolymph-filled space is also formed between the dorsal diaphragm and the gut (Fig. 1D). The dorsal diaphragm ceases up to the eighth segment. The hepatopancreas is composed of four tubules that become thinner and terminate approximately at segments nine or ten along with the midgut entering the rectum. Together, these anatomical features result in the formation of a substantial lacuna approximately from the anterior part of the eighth to the anterior part of the tenth segment (Fig. 1B).

The size of these hemolymph-filled spaces was found to be highly dependent on two main factors. First, the digestive activity of the individual can substantially influence the volume of lacuna under the dorsal diaphragm. The second factor specifically for females is reproductive season. The male reproductive organs, the seminal vesicles, are located under the diaphragm from the third to the seventh segment (Fig. 1A). In females, oocyte vitellogenesis occurs during the reproductive period in the gonads that are

located in the space between the intestine and the diaphragm from the third to the eighth or ninth segment (Fig. 1F). Thus, the space decreases significantly as the oocytes mature, and the space at the ninth segment can also be affected (Fig. 1E).

Interestingly, both males and females of *E. verrucosus* demonstrated accumulations of lipid droplets on the hepatopancreas ducts mostly during the reproductive season (Fig. 1C,E). The droplets are approximately 7–100 μm in diameter, vary from having red color to no coloration and have no internal structure (Fig. 3). Individual analysis revealed that these clusters appear to be structurally linked by connective tissue to the hepatopancreas ducts and intestine, rather than just being adjacent.

Structure of carinae of *Acanthogammarus* amphipods

Optical sensors in deep tissues of amphipods, which are significantly larger than *E. verrucosus*, are practically impossible to visualize due to light scattering. However, the sensors may still be applied close to the surface in muscles or other organs. Intriguing body parts in this context

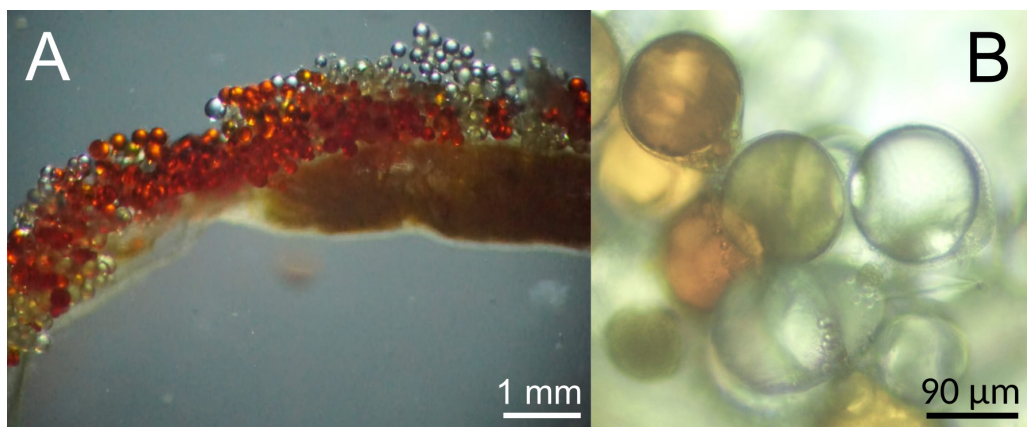


Fig. 3. Lipid droplets extracted from *Eulimnogammarus verrucosus* ($n = 3$). A — general view of intestine with lipid droplets; B — enlarged view of lipid droplets in the connective tissue.

are various outgrowths of exoskeleton such as dorsal carinae. In order to analyze the anatomy of deeper-dwelling animals and their carinae specifically, we initially chose *A. grewingkii*, the largest (Takhteev, 2000) amphipod species in Lake Baikal (Fig. 4A).

The deep-water species *A. grewingkii* is several times larger than littoral *E. verrucosus* but has generally similar anatomy despite some peculiarities such as large coxal plates with projections or highly developed musculature, including apical muscles (Fig. 4). The presence of carinae, i.e. outgrowths on the dorsal side, is one of its distinguishing characteristics, and the largest carinae are observed in segments from the seventh to ninth. Morphologically at their base the carinae are approximately 1 mm thick (Fig. 4B). However, anatomically the tissue inside carina also covers most of the animal's dorsal surface under its exoskeleton and is separated from apical muscles by another layer of chitinous cuticle (Fig. 4C,D). The tissue inside carinae is similar to adipose tissue by its histological structure (Fig. 4D,E) and seemingly contains some hemocytes, i.e. the immune cells mostly concentrating in the hemolymph (Fig. 4F). Similarly to *E. verrucosus*, we also observed lipid droplets in ovigerous females *A. grewingkii* (only those were subjected to cryotomy), but in this species they were located laterally in segments from the third to the fifth (Fig. 4B).

The internal chitinous structure on *A. grewingkii* transverse sections raised the obvious question of how it is formed by the exoskeleton.

Unfortunately, we were not able to obtain more samples of this species for longitudinal sectioning and had to use to another species of the same genus, *A. victorii*. Histological analysis showed the same anatomy of carinae on transverse sections (Fig. 5C,D) and revealed that the chitinous structure separating adipose-like tissue inside carina from apical muscles is a simple fold of amphipod exoskeleton (Fig. 5A,B).

Optical features of amphipod tissues

The optimal organs for application of optical sensors should have minimal autofluorescence and maximal translucency of tissues and exoskeleton. Since previously we externally observed intense autofluorescence of some internal organs of *E. verrucosus* (Shchapova *et al.*, 2019) but the current study revealed significant hemolymph-filled spaces in pereon of the species as potential implantation sites, we decided to search for the exact sources of autofluorescence using cryosections. Exoskeleton of the species generally had low autofluorescence with exceptions to spines and setae on urosome (Fig. 6B). Previously we had hypothesized that autofluorescence of internal organs was mostly due to intestine (Shchapova *et al.*, 2019), but it turned out to be also caused by hepatopancreas ducts (Fig. 6A).

Next, in order to evaluate the applicability of fluorescent sensors in larger amphipods with markedly more substantial exoskeleton, we again chose *A. victorii* as the species that could be relatively easily collected and brought alive to laboratory. We visualized filamentous hydrogels

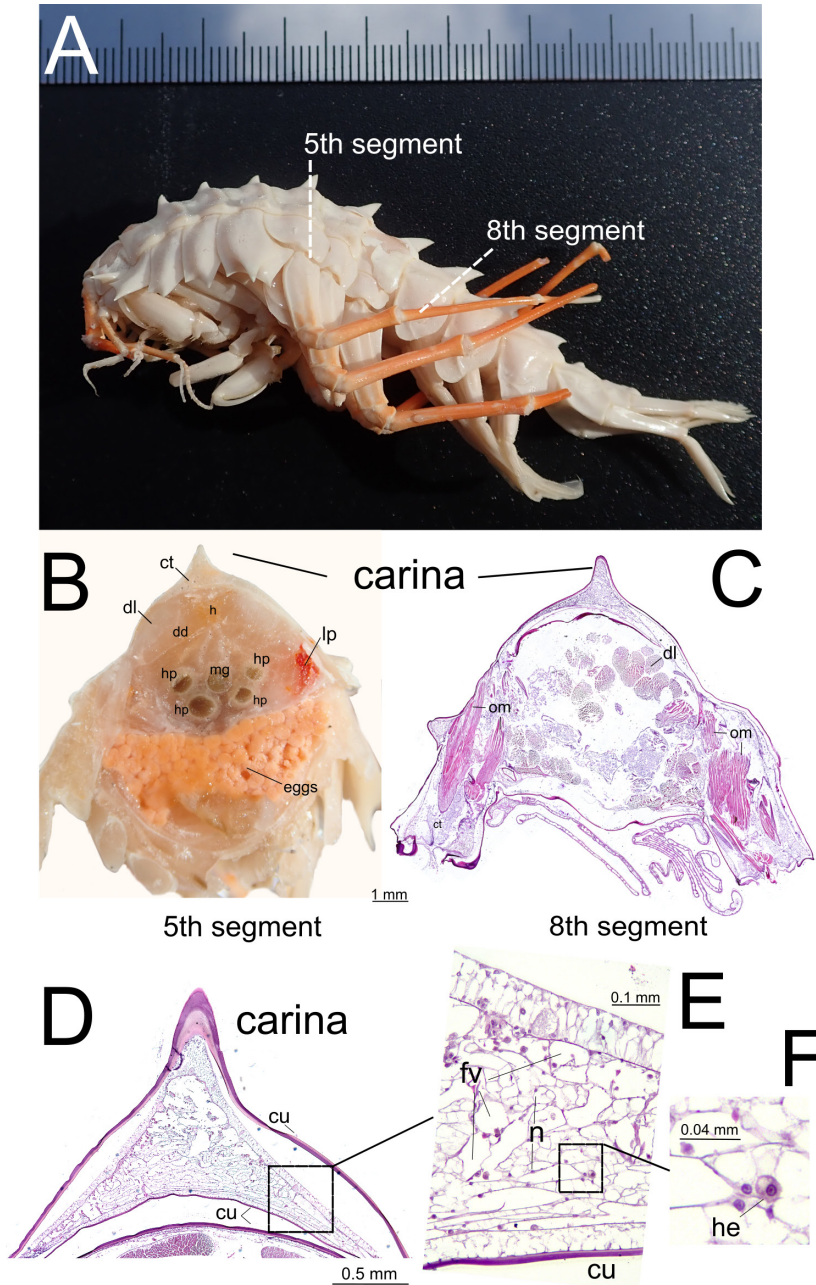


Fig. 4. Anatomy of *Acanthogammarus grewingkii*. A — general view of fixed *Acanthogammarus grewingkii*, the dashed lines show the cross sections; B — transverse cryosection of the fifth segment of *Acanthogammarus grewingkii* ($n = 5$); C–F — transverse histological section of the eighth segment of pleon stained with H&E ($n = 3$); C — general view of the eighth segment; D, E, F — general structure of the carina and tissue in the carina.

Abbreviations: ct — adipose connective tissue; cu — cuticle; dd — dorsal diaphragm; dl — dorsal longitudinal (apical) muscle; fv — fat vacuole; h — lumen of the heart; he — putative hemocyte; lp — lipid droplets; mg — midgut; n — nucleus of adipose connective tissue; om — oblique muscle. Scale bars: A — the major scale on the ruler is 1 cm.

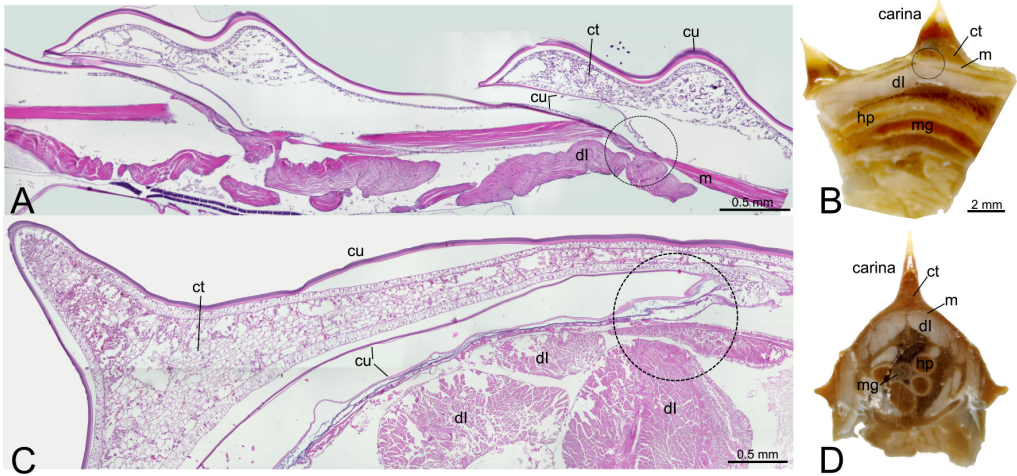


Fig. 5. Anatomy of *Acanthogammarus victorii*. A — longitudinal histological section of the eighth and ninth segments of the pleone stained with H&E ($n = 2$); B — longitudinal cryosection of the eighth and ninth segments of the pleone ($n = 3$); C — transverse histological section of the fifth segment of pereon stained with H&E ($n = 2$); D — transverse cryosection of the fifth segment of pereon ($n = 2$). The scale bar is identical for B and D.

Abbreviations: ct — adipose connective tissue; cu — cuticle; dl — dorsal longitudinal (apical) muscle; m — muscle; mg — mid-gut; hp — hepatopancreas.

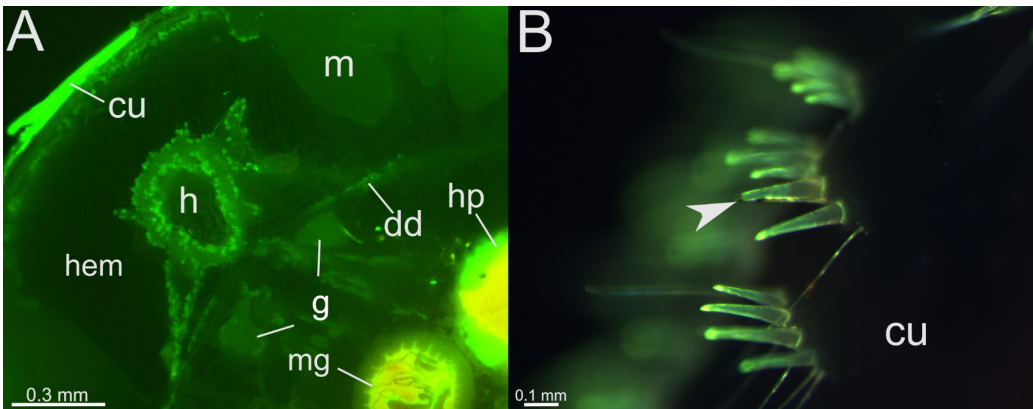


Fig. 6. Autofluorescence of *Eulimnogammarus verrucosus*. A — transverse cryosection of the fifth segment ($n = 8$); B — spines (indicated with the arrowhead) and setae on pleon of alive amphipod ($n = 3$). Overlays of red and green fluorescent channels.

Abbreviations: cu — cuticle; dd — dorsal diaphragm; g — gonads; h — lumen of the heart; hem — hemolymph; hp — hepatopancreas; mg — mid-gut; m — muscle.

carrying a substantial amount of the pH-sensitive fluorescent dye SNARF-1 after injecting them under the exoskeleton into the apical muscles of both *E. verrucosus* and *A. victorii* (Fig. 7). Surprisingly, exoskeleton autofluorescence of the fifth and sixth segments of not only *E. verrucosus* but also *A. victorii* was found to be negligible in

the comparison to the sensor fluorescence. Quantitative comparison showed that exoskeleton and tissues of *E. verrucosus* reduced the registered sensor fluorescence intensity about three times in comparison to free gels, and in case of *A. victorii* the decrease was approximately tenfold. Thus, the difference in light transmittance at ~600 nm

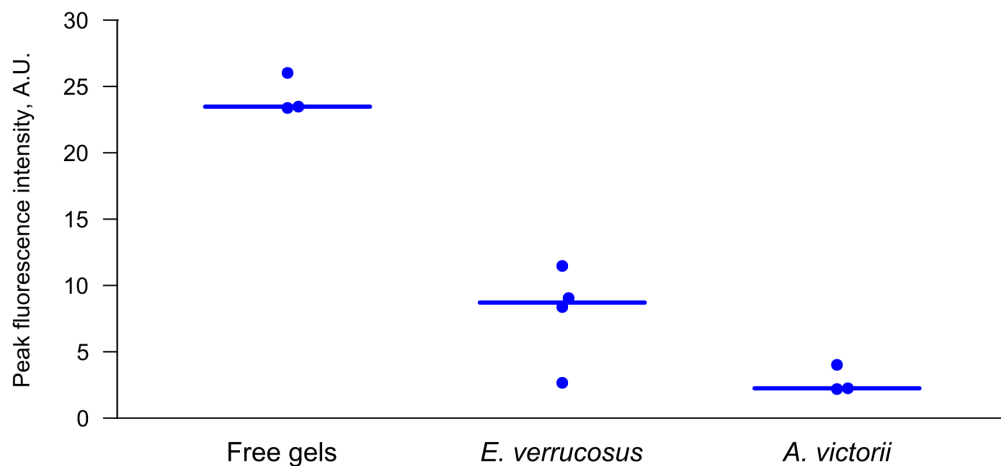


Fig. 7. Fluorescence intensities of the sensory gels containing SNARF-1 in the apical muscles in fifth-sixth segments of *Eulimnogammarus verrucosus* and *Acanthogammarus victorii*. Each dot represents individual amphipod and the lines show medians.

between two species was indeed substantial but the sensor fluorescence was still visible by eye and detectable by spectrometer for *A. victorii*.

Discussion

Implants may have different purposes dictating their injection sites for either systemic or local tissue application. An unexpected finding of the study was the observation of numerous lipid droplets both in littoral *E. verrucosus* and deep-water *A. grewingkii* at least in certain conditions (Figs 1, 4), which might be potential sites for targeted release of hormones or other hydrophobic compounds. Such localized delivery may be beneficial for increasing bioavailability of these compounds (Shrestha *et al.*, 2014) during cultivation or research on amphipods. Even a more easily accessible site for slow release of hydrophobic compounds specifically in the case of *Acanthogammarus* may be their carinae, as we found a substantial amount of adipose-like tissue under the dorsal part of their exoskeleton (Fig. 4). However, the rate of further diffusion from these two types of structures to other tissues is now completely unpredictable and may be restricting for such application, especially in the case of adipose-like tissue in carinae due to the exoskeleton fold partially separating it from the rest of the body. The last concern is equally relevant for application of implantable sensors in carinae of *A. victorii* and similar species.

Fortunately, we found that implantable optical sensors can be used even simply in muscles of larger amphipods on the example of *A. victorii* (Fig. 7), which is morphologically similar to *A. grewingkii*. Thus, apical muscles on either side from the sagittal body plane (Fig. 2,4) can be equally used for monitoring of tissue physiology both in relatively small amphipods as we previously showed for *E. verrucosus* (Nazarova *et al.*, 2023) and in large species as we showed here. Moreover, to our experience, these muscles are the most realistic site for safe injections into even smaller species of ~1 cm long, such as adults of important crustacean model *Parhyale hawaiiensis* (Dana, 1853) (Paris *et al.*, 2022). If such injections are practically feasible, it would make apical muscles the most universal site for implantation of optical sensors in amphipods of different sizes.

However, our main focus with smaller amphipods in this study was the search for potential sites where the implant may have direct contact with hemolymph for most prompt monitoring of physiological changes in the organism or adjustments with drug release. Previously when we injected fluorescent microcapsules into the hemolymph of *E. verrucosus* (Gurkov *et al.*, 2016; Shchapova *et al.*, 2019), we supposed that the microcapsules mostly settled in the dorsal vessel (or central hemolymph vessel; i.e. heart with aortae) and probably numerous smaller lacunae between organs, as we relied on most available

schematics concentrating around the circulatory system (Wirkner, Richter, 2007; Wirkner *et al.*, 2013). Frozen sectioning of *E. verrucosus* showed it is the other way around with the main lacunae being much larger than the dorsal vessel, and in some cases the microcapsules could have been observed previously from those cavities and not from the vessel. We found three main hemolymph-filled spaces in *E. verrucosus*: two above and under the dorsal diaphragm and the united one from the ninth segment where the diaphragm ends (Fig. 1). The space under the dorsal diaphragm is the least promising in the context of optical sensors due to light scattering by surrounding organs, intense autofluorescence of both intestine and hepatopancreas (Fig. 6), variable volume depending on digestive activity and oocyte vitellogenesis in females (Fig. 1), as well as high risk of damaging the internal organs during the injection.

On the contrary, the other two spaces may have specific applications defined by their distinct features. The space above the dorsal diaphragm is relatively small, and there is a risk of damaging the heart during the injection into this space (Fig. 6). Thus, large sensors or implants for drug release (over $\sim 100\ \mu\text{m}$ in diameter) are hardly applicable here, but in the case of smaller structures such as microcapsules ($\sim 4\ \mu\text{m}$ in diameter) this dorsal lacuna is even preferred over the dorsal vessel since the microcapsules should settle here immediately and not distribute further around the body so intensely. The microcapsules are sometimes better suited as carriers for specific sensors, for example, due to faster response times in comparison to hydrogel fibers. The transversal sections obtained in this study (Fig. 6) also suggest that fluorescent microcapsules in the dorsal part of the body should be visualized from above the amphipod and not from its side as we did previously (Gurkov *et al.*, 2016) since in the latter case the light is highly scattered by apical muscles. However, due to small size, the microcapsules are faster affected by the animal immune system (Shchapova *et al.*, 2019) and larger sensory implants are usually preferred.

The highest potential for application of different implants specifically in amphipod hemolymph is probably related to the large posterior lacuna that was found in the ninth-tenth segments of *E. verrucosus* (Fig. 1). The risk of damaging internal organs is minimal with injecting large

implants ($\sim 300\ \mu\text{m}$ in diameter) in this space. The only apparent drawback of this site for application of optical sensors is high autofluorescence of sclerotized armor (Fig. 5) as we briefly mentioned previously (Shchapova *et al.*, 2019), but it can be avoided by using non-fluorescent sensors or complex sensors with infrared excitation and visible luminescence (Nazarova *et al.*, 2023).

An unexpected finding of our study that deserves further anatomical research was the internal fold of exoskeleton separating the adipose-like tissue from muscles in the carinae of *Acanthogammarus* amphipods. The overall structure resembles by form the hump of camels used for nutrient storage (Endo *et al.*, 2000) and may have similar function in Baikal amphipods. It is yet unclear where the tissues inside carina are connected to the rest of the living tissues for hemolymph inflow and how those structures of carinae develop during ontogeny.

Conclusion

This study resolved the major remaining questions about application of implantable sensors in amphipods of different sizes. When the implants must be in direct contact with hemolymph of middle-sized animals similar to *E. verrucosus* ($\sim 2\text{--}4\ \text{cm}$ in length), the injections can be performed into the large lacuna in the ninth-tenth segments if the sensors are large ($\sim 300\ \mu\text{m}$ thick) or into the lacuna above dorsal diaphragm if the sensors should be smaller due to any reason (up to $\sim 50\ \mu\text{m}$). The most universal implantation site for amphipods of various sizes seems to be the apical muscles, specifically their parts located laterally from the sagittal body plane. Additionally, here we also found adipose-like tissue in carinae of *A. grewingkii* and *A. victorii* separated from apical muscles by internal fold of chitinous exoskeleton that deserves further anatomical research.

Compliance with ethical standards

CONFLICTS OF INTEREST: All authors declare that they have no conflicts of interest.

Data availability statement

The obtained data are available within the manuscript or through the related open repository at https://figshare.com/projects/Anatomy_of_endemic_amphipods_from_Lake_Baikal/223560

Acknowledgements

We sincerely thank divers Yulia Mikhaleva and Andrey Dimitrevich for their assistance in collecting *A. victorii*. Special thanks to Dr. Ekaterina Govorukhina, who kindly helped in identifying the species. We also thank Dr. Polina Drozdova, as well as three anonymous reviewers for valuable suggestions and corrections along the whole manuscript. The study was supported by the Russian Science Foundation within the project #24-74-00095 (<https://rscf.ru/en/project/24-74-00095/>).

References

- Ahyong S.T., Lowry J.K., Alonso M., Bamber R.N., Boxshall G.A., Castro P., Gerken S., Karaman G.S., Goy J.W., Jones D.S., Meland K., Rogers D.C., Svavarsson J. 2011. Subphylum Crustacea Brünnich, 1772 // Zhang Z.-Q. (ed.). Animal biodiversity: An outline of higher-level classification and survey of taxonomic richness. Zootaxa. Vol.3148. No.1. P.165–191.
- Bazikalova A.Y. 1945. [Amphipods of Lake Baikal] // Trudy Baikal'skoy limnologicheskoy stantsii. Vol.11. P.1–440 [in Russian].
- Bellan-Santini D. 2015. Order Amphipoda Latreille, 1816 // Treatise on Zoology-Anatomy, Taxonomy, Biology. The Crustacea. Vol.5. Brill. P.93–248.
- Bhoi G., Dubey S.K., Patro S. 2023. Marine benthic amphipods (Amphipoda) of India: an assessment on their biodiversity, distribution and significance // Thalassas: An International Journal of Marine Sciences. Vol.39. P.215–233.
- Drozdova P., Saranchina A., Morgunova M., Kizenko A., Lubyaga Y., Baduev B., Timofeyev M. 2020. The level of putative carotenoid-binding proteins determines the body color in two species of endemic Lake Baikal amphipods // PeerJ. Vol.8. Art.e9387.
- Ehrlich R., Hendlar-Neumark A., Wulf V., Amir D., Bisker G. 2021. Optical nanosensors for real-time feedback on insulin secretion by β -cells // Small. Vol.17. Art.2101660.
- Endo H., Cao G. F., Borjihan D., Borjihan E., Dugarjav M., Hayashi Y. 2000. Hump attachment structure of the two-humped camel (*Camelus bactrianus*) // Journal of Veterinary Medical Science. Vol.62. No.5. P.521–524.
- Gudlavalleti R.H., Xi X., Legassey A., Chan P.Y., Li J., Burgess, D., Giardina C., Papadimitrakopoulos F., Jain F. 2024. Highly miniaturized, low-power CMOS ASIC chip for long-term continuous glucose monitoring // Journal of Diabetes Science and Technology. Vol.18. No.5. P.1179–1184.
- Gurkov A., Borvinskaya E., Shchapova E., Timofeyev M. 2018. Restraining small decapods and amphipods for *in vivo* laboratory studies // Crustaceana. Vol.91. P.517–525.
- Gurkov A., Shchapova E., Bedulina D., Baduev B., Borvinskaya E., Meglinski I., Timofeyev, M. 2016. Remote *in vivo* stress assessment of aquatic animals with microencapsulated biomarkers for environmental monitoring // Scientific Reports. Vol.6. Art.36427.
- Hu C., Wang L., Liu S., Sheng X., Yin L. 2024. Recent development of implantable chemical sensors utilizing flexible and biodegradable materials for biomedical applications // ACS Nano. Vol.18. P.3969–3995.
- Hyne R.V. 2011. Review of the reproductive biology of amphipods and their endocrine regulation: identification of mechanistic pathways for reproductive toxicants // Environmental toxicology and chemistry. Vol.30. P.2647–2657.
- Ivich F., Calderon I., Fang Q., Clark H., Niedre M. 2023. Ratiometric fluorescence sensing and quantification of circulating blood sodium sensors in mice *in vivo* // Biomedical Optics Express. Vol.14. P.5555–5568.
- Kaefler K., Kruger K., Schlapp F., Uzun H., Celiksoy S., Flietel B., Heimann A., Schroeder T., Kempfski O., Sonnichsen C. 2021. Implantable sensors based on gold nanoparticles for continuous long-term concentration monitoring in the body // Nano Letters. Vol.21. P.3325–3330.
- Kanick S.C., Schneider P.A., Klitzman B., Wisniewski N.A., Rebrin K. 2019. Continuous monitoring of interstitial tissue oxygen using subcutaneous oxygen microsensors: *In vivo* characterization in healthy volunteers // Microvascular research. Vol.124. P.6–18.
- Kozhov M. 1963. Lake Baikal and its life. Dordrecht: Springer. Vol.11.
- Li P., Lee G.H., Kim S.Y., Kwon S.Y., Kim H.R., Park S. 2021. From diagnosis to treatment: recent advances in patient-friendly biosensors and implantable devices // ACS Nano. Vol.15. P.1960–2004.
- Madhu N., Das P., Yellurkar M.L., Prasanna V.S., Chandran, A., Kumar B., Sarkar S., Velayutham R., Sreedhar R., Arumugam S. 2024. Implantable biosensor platforms for animal model bioassays // M. Veerapandian, J. Joseph, M. Marimuthu (eds.). Health and Environmental Applications of Biosensing Technologies. Elsevier. P.181–199.
- McCallum E.S., Cervený D., Fick J., Brodin T. 2019. Slow-release implants for manipulating contaminant exposures in aquatic wildlife: a new tool for field ecotoxicology // Environmental Science & Technology. Vol.53. P.8282–8290.
- Mekhanikova I.V., Andreev D.S., Belozeroва O.Y., Mikhlin Y.L., Lipko S.V., Klimenkov I.V., Akimov V.V., Kargin V.F., Mazurova Y.V., Tauson V.L., Likhoshvay Y.V. 2012. Specific features of mandible structure and elemental composition in the polyphagous amphipod *Acanthogammarus grewingkii* endemic to Lake Baikal // PLoS ONE. Vol.7. No.8. Art.e43073.
- Nazarova A., Gurkov A., Rzhchitskiy Y., Shchapova E., Mutin A., Saranchina A., Diagileva A., Bolbat N., Krivoshapkin P., Timofeyev M. 2023. Turn a shrimp into a firefly: Monitoring tissue pH in small crustaceans using an injectable hydrogel sensor with infrared excitation and visible luminescence // Photonics. Vol.10. No.6. Art.697.
- Paris M., Wolff C., Patel N.H., Averof M. 2022. The crustacean model *Parhyale hawaiensis* // Current Topics in Developmental Biology. Vol.147. P.199–230.
- Rabet N. 2021. Crustaceans // A. Boutet, B. Schierwater (eds.). Handbook of Marine Model Organisms in Experimental Biology. Boca Raton: CRC Press. P.271–287.
- Ramm T., Scholtz G. 2017. No sight, no smell? – Brain anatomy of two amphipod crustaceans with different lifestyles // Arthropod Structure & Development. Vol.46. P.537–551.
- Rzhchitskiy Y., Gurkov A., Bolbat N., Shchapova E., Nazarova A., Timofeyev M., Borvinskaya E. 2022. Adipose fin as a natural “optical window” for implanta-

- tion of fluorescent sensors into salmonid fish // *Animals*. Vol.12. Art.3042.
- Schmitz E.H. 1967. Visceral anatomy of *Gammarus lacustris lacustris* Sars (Crustacea: Amphipoda) // *The American Midland Naturalist*. Vol.78. P.1–54.
- Schneider C.A., Rasband W.S., Eliceiri K.W. 2012. NIH Image to ImageJ: 25 years of image analysis // *Nature Methods*. Vol.9. P.671–675.
- Shchapova E., Nazarova A., Gurkov A., Borvinskaya E., Rzhechitskiy Y., Dmitriev I., Meglinski I., Timofeyev M. 2019. Application of PEG-covered non-biodegradable polyelectrolyte microcapsules in the crustacean circulatory system on the example of the amphipod *Eulimnogammarus verrucosus* // *Polymers*. Vol.11. Art.1246.
- Shchapova E., Titov E., Gurkov A., Nazarova A., Borvinskaya E., Timofeyev M. 2022. Durability of implanted low-density polyacrylamide hydrogel used as a scaffold for microencapsulated molecular probes inside small fish // *Polymers*. Vol.14. Art.3956.
- Shrestha H., Bala R., Arora S. 2014. Lipid-based drug delivery systems // *Journal of Pharmaceutics*. Vol.2014. Art.801820.
- Sonmezoglu S., Fineman J.R., Maltepe E., Maharbiz M.M. 2021. Monitoring deep-tissue oxygenation with a millimeter-scale ultrasonic implant // *Nature Biotechnology*. Vol.39. P.855–864.
- Takhteev V.V. 2000. [Essays on amphipods of Lake Baikal: Systematics, comparative ecology, evolution]. Irkutsk: Irkutsk State University Press. 355 p. [In Russian]
- Takhteev V.V., Berezina N.A., Sidorov D.A. 2015. [Checklist of the Amphipoda (Crustacea) from continental waters of Russia, with data on alien species] // *Arthropoda Selecta*. Vol.24. P.335–370 [in Russian].
- Wirkner C.S., Richter S. 2007. Comparative analysis of the circulatory system in Amphipoda (Malacostraca, Crustacea) // *Acta Zoologica*. Vol.88. P.159–171.
- Wirkner C.S., Togel M., Pass G. 2013. The arthropod circulatory system // A. Minelli, G. Boxshall, G. Fusco (eds.). *Arthropod Biology and Evolution: Molecules, Development, Morphology*. Heidelberg: Springer. P.343–391.
- Wittfoth C., Harzsch S., Wolff C., Sombke A. 2019. The “amphi”-brains of amphipods: new insights from the neuroanatomy of *Parhyale hawaiiensis* (Dana, 1853) // *Frontiers in Zoology*. Vol.16. P.1–20.

Responsible editor: E.N. Temereva